4-5 Time Comparison Equipment for ETS-Ⅷ Satellite —Part 2 Plans of Precise Time Transfer Experiment—

GOTOH Tadahiro, HOSOKAWA Mizuhiko, NAKAGAWA Fumimaru, TAKAHASHI Yasuhiro, FUJIEDA Miho, IMAE Michito, KIUCHI Hitoshi, AIDA Masanori, and TAKAHASHI Yukio

Engineering Test Satellite Ⅷ (ETS-Ⅷ), which is planed to launch in 2004 will carry a highly precise cesium clock system on its mission first time in Japan for fundamental studies. To estimate precision of this clock, CRL has developed highly precise time comparison equipment. This one can measure the clock offsets between satellite and the Earth stations with precision of a few nanoseconds by code observations and of a few picoseconds by carrier phase observations.

Using this equipment via the ETS-Ⅷ not only provides advanced time-transfer technologies between space and the Earth, but also gives highly precise time-transfer between each Earth stations as well as a possibility for comparing ranging technology between radio and laser signals.

Keywords
ETS-Ⅷ, Satellite navigation, Time transfer

1 Introduction

The Engineering Test Satellite Ⅷ (ETS-Ⅷ)[1] due to be launched in 2004 was designed to develop the advanced common base technology required for future space activities. Equipment aboard the satellite will include a large expandable antenna for mobile communication experiments, a corner cube reflector (CCR) for satellite laser ranging (SLR) to acquire advance satellite navigation technology, and a cesium atomic clock (a Highly Accurate Clock, or HAC).

The CRL will provide onboard time comparison equipment (TCE) capable of performing highly precise time transfer between the satellite and the ground and will evaluate the performance of the atomic clock in orbit[2]. While the well-known LASSO experiment carried out in the 1980s[3][4] evaluated the performance of an on-board clock using an SLR station, the TCE and TCE Earth stations will evaluate the performance of the on-board clock by the two-way time transfer method[5]. In this evaluation, the carrier phase can be used as an observed value in addition to the pseudo-ranging, and thus comparison precision within a few tens of ps may be expected. Moreover, since the satellite and the Earth station each transmit signals to the other, almost the same observed values can be directly obtained using radio waves as obtained by using an SLR station.

In addition to a fixed station, a portable TCE Earth station will be developed. Through this arrangement, time transfer via TCE becomes possible both between a satellite and an Earth station and between Earth stations. In two-way satellite time transfer using a communication satellite, a satellite oscillator proves unstable, and therefore time transfer is only possible using the pseudo random noise (PRN) code. In cases in which TCE is used as an intermediary, the carrier phase may also be used, resulting in more highly precise time transfer relative to two-way satellite time transfer via communication satellite.

2 Time transfer system

2.1 System configuration

The fundamental theory behind TCE is described in detail elsewhere in this journal [2]. Here we will provide a brief explanation of the principle of time transfer using TCE. The time transfer system consists of a HAC system, a main TCE component aboard the satellite, and two TCE Earth stations on the ground (Fig.1).

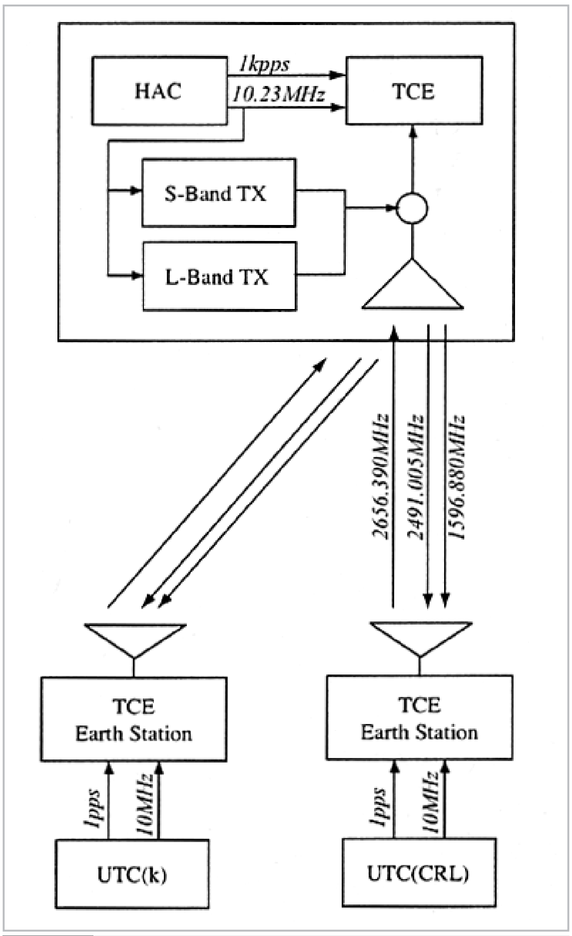

Fig. 1 Configuration of the time transfer system using TCE and TCE Earth stations

The reference signal of TCE Earth station is based on UTC(CRL), while TCE operates using reference signals of 1 kpps and 10.23 MHz supplied from HAC. The S-band is used for time transfer transmission and reception signals; the Earth station transmission frequency is 2,656.390 MHz, and the satellite transmission frequency is 2,491.005 MHz. Both transmitting signals are superposed on a ranging signal that is modulated using the spread-spectrum method with a chip rate of 1.023 MHz. For the spreading code, the same type of pseudo random noise (PRN) employed in the C/A code of the GPS is used. It is thus possible to perform time transfer using two kinds of observed values—pseudo range and carrier phase—as in the case of GPS. Additionally, to perform ionospheric correction, an L-band (1,595.880 MHz) signal is sent, albeit unidirectionally (from the satellite to the ground).

In addition to the receipt of a signal from the ground, TCE receives a transmitting signal and a calibration signal from the satellite, allowing for real-time monitoring of variation in internal delay. The units that receive these three types of signals feature the same configuration; each unit processes a signal whose frequency has been down-converted to an IF. Modification of the PRN code therefore allows for simultaneous receipt from three Earth stations, permitting two-way satellite time transfer between Earth stations via TCE.

2.2 Observed value

Observed values for code phase and carrier phase measured by the TCE and the Earth stations can be expressed as they are under GPS, although the frequencies will differ[6]. The observed value of the code phase is expressed by the following.

$$\begin{aligned} C_r(t) &= \|[\boldsymbol{r}^s(t-\tau_r)+d\boldsymbol{r}^s(t-\tau_r)]-[\boldsymbol{r}_r(t)+d\boldsymbol{r}_r(t)]\| \\ &\quad +I_d+T+c[dt_r(t)-dt^s(t-\tau_r)] \\ &\quad +c[d_{rr}(t)+d^s_s(t-\tau_r)]+e_r \qquad (1) \end{aligned}$$

$$\begin{aligned} C^s(t) &= \|[\boldsymbol{r}_r(t-\tau^s)+d\boldsymbol{r}_r(t-\tau^s)]-[\boldsymbol{r}^s(t)+d\boldsymbol{r}^s(t)]\| \\ &\quad +I_u+T+c[dt^s(t)-dt_r(t-\tau_r)] \\ &\quad +c[d^s_r(t)+d_{sr}(t-\tau_r)]+e^s \qquad (2) \end{aligned}$$

Here, C_r, C^s-represents the code phases received by the Earth station and the satellite, respectively, in units of distance (m); τ_r, τ^s-

stands for propagation times from the Earth station to the satellite and from the satellite to the Earth station; $\boldsymbol{r}^s, d\boldsymbol{r}^s$-is the position vector of the center-of-mass and the eccentricity vector of the satellite antenna; $\boldsymbol{r}_r, d\boldsymbol{r}_r$-is the position vector of the terrestrial point and the eccentricity vector of the station antenna; T-stands for tropospheric delay; I_u, I_d-represent ionospheric delays for UPLINK and for DOWNLINK, respectively; dt_r, dt^s-represents the clock offsets of the Earth station and of the satellite; d_{rr}, d_r^s-are receiver's internal delays of the Earth station and of the satellite; and d_{sr}, d_s^s-represent transmitter's internal delays of the Earth station and of the satellite.

A significant difference between TCE and the GPS receiver is that the GPS is capable of measuring a pseudo range between the satellite and the receiver, whereas TCE has no time information besides 1 kpps and thus outputs the code phase as a measured value. Therefore, the code phase has an initial phase ambiguity, as in the case of the carrier phase. However, the period of the ambiguity may be as large as 1 ms. When performing time transfer, the code phase ambiguity can be ignored because the offset between the satellite and Earth clocks feature a minimal offset—rarely more than 1 ms.

To perform time transfer, the difference between the two observed values is determined.

$$
\begin{aligned}
C_r(t) - C^s(t) \;=\; & \{\|[\boldsymbol{r}^s(t-\tau_r) + d\boldsymbol{r}^s(t-\tau_r)] - [\boldsymbol{r}_r(t) + d\boldsymbol{r}_r(t)]\| \\
& - \|[\boldsymbol{r}_r(t-\tau^s) + d\boldsymbol{r}_r(t-\tau^s)] - [\boldsymbol{r}^s(t) + d\boldsymbol{r}^s(t)]\|\} \\
& + \{I_d - I_u\} \qquad\qquad (3) \\
& + c\{[dt_r(t) - dt^s(t-\tau_r)] - [dt^s(t) - dt_r(t-\tau_r)]\} \\
& + c\{[d_{rr}(t) + d_s^s(t-\tau_r)] - [d_r^s(t) + d_{sr}(t-\tau_r)]\} + e_r^s
\end{aligned}
$$

Since ETS-Ⅷ will be placed in geostationary orbit, and since the satellite and the Earth station transmit signals simultaneously, the distance the satellite moves at this moment is small and can be regarded as $\tau_r \simeq \tau^s$. Moreover, if the distance between the satellite and the Earth station is taken into consideration, calculation can be performed safely assuming that the satellite moves a distance of $\boldsymbol{r}^s(t-\tau_r) \simeq \boldsymbol{r}^s(t)$, $\boldsymbol{r}_r(t-\tau^s) \simeq \boldsymbol{r}_r(t)$. τ_r, τ^s may be as large as approximately 100 ms, $dt_r(t) \simeq dt_r(t-\tau^s)$, $dt^s(t) \simeq dt^s(t-\tau_r)$ is assumed. Moreover, the internal delay is expressed by $d_r = d_{rr} - d_{sr}$, $d^s = d_r^s - d_s^s$, and formula (3) can be rewritten simply as formula (4).

$$
\begin{aligned}
C_r(t) - C^s(t) \;=\; & 2c(dt_r - dt^s) + c(d_r - d^s) \\
& + (I_d - I_u) + e_r^s \qquad (4)
\end{aligned}
$$

In formula (4), if the internal delay and the ionospheric delay can be separately determined, the time difference between the satellite and the Earth station can be found. Similarly to the expression of the code phase, the carrier phase can be expressed as follows.

$$
\begin{aligned}
\Phi_r(t) \;=\; & \|[\boldsymbol{r}^s(t-\tau_r) + d\boldsymbol{r}^s(t-\tau_r)] - [\boldsymbol{r}_r(t) + d\boldsymbol{r}_r(t)]\| \\
& - I_d + T + c[dt_r(t) - dt^s(t-\tau_r)] \\
& + c[\delta_{rr}(t) + \delta_s^s(t-\tau_r)] \qquad (5) \\
& + \lambda_d[\phi_r(t_0) - \phi^s(t_0)] + \lambda_d N_r + \varepsilon_r \\
\Phi^s(t) \;=\; & \|[\boldsymbol{r}_r(t-\tau^s) + d\boldsymbol{r}_r(t-\tau^s)] - [\boldsymbol{r}^s(t) + d\boldsymbol{r}^s(t)]\| \\
& - I_u + T + c[dt^s(t) - dt_r(t-\tau_r)] \\
& + c[\delta_r^s(t) + \delta_{sr}(t-\tau_r)] \\
& + \lambda_u[\phi^s(t_0) - \phi_r(t_0)] + \lambda_u N^s + \varepsilon^s \qquad (6)
\end{aligned}
$$

Ionospheric delay of the carrier phase is reversed in sign relative to the sigh of the code phase because ionospheric delay has changed from group delay to phase delay. Internal equipment delay in this case is not identical to that of the code phase, and so the delay is expressed by δ instead of d. The carrier phase has additional terms: the initial phase ($\phi_r(t_0)$, $\phi^s(t_0)$), and integer carrier phase ambiguity (N_r, N^s). Since error becomes smaller than that of the code phase, ε is used to express the error independently.

Also in the case of the carrier phase, the time difference can be determined as follows using the same variables used for the code phase.

$$
\begin{aligned}
\Phi_r(t) - \Phi^s(t) \;=\; & 2c(dt_r - dt^s) + c(\delta_r - \delta^s) - (I_d - I_u) \\
& + \lambda_d[\phi_r(t_0) - \phi^s(t_0) + N_r] \\
& - \lambda_u[\phi^s(t_0) - \phi_r(t_0) + N^s] \\
& + \varepsilon_r^s \qquad (7)
\end{aligned}
$$

Since the period of the carrier phase may be as short as approximately 400 ps, carrier phase ambiguity cannot be ignored, as in the case of the code phase. For this reason, when performing time transfer using the carrier phase, it is necessary to resolve ambiguity in one manner or another.

2.3 Time transfer precision

2.3.1 System noise

In order to evaluate the system noise of TCE, Engineering model (EM2) was used to conduct the characteristic test shown in Fig.2.

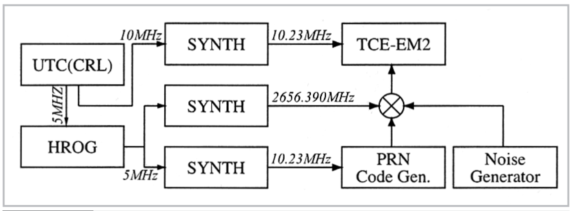

Fig.2 *System configuration for measurement of system noise in the engineering model (EM2)*

"HROG" in the figure represents an apparatus used to shift the phase and frequency of the reference frequency in minute amounts. In this experiment, the frequency is shifted by 3×10^{-6}Hz to 5MHz of UTC(CRL) to perform the measurement. Moreover, in order to simulate the signal from the actual satellite, white noise was added by a noise generator in measurement. In this experiment, noise of approximately $C/N_0 \simeq 54$dB was introduced. Note that in actual experiments, line quality of more than 65 dB is expected.

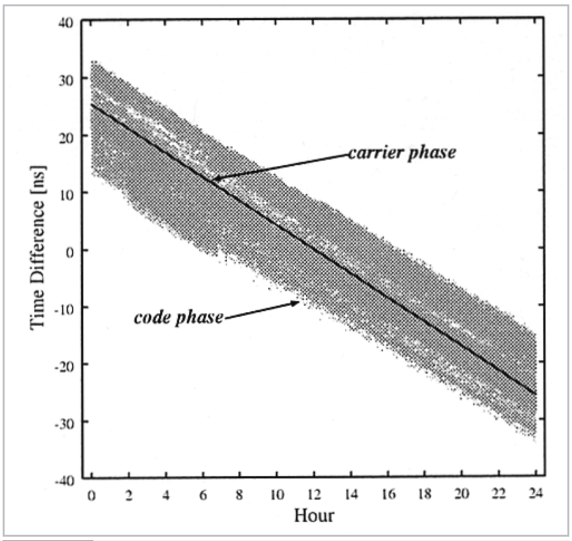

Fig.3 *Results obtained by EM2 measurement of a frequency shifted by HROG by 3×10^{-6}*

Plots having large dispersion represent results using the code phase, and the nearly straight-line plots in the center represent results using the carrier phase.

Fig.3 shows the measurement results for the code phase and the carrier phase, and Fig. 4 shows the residual of the carrier phase after the least-square linear fit. The slope estimated by this method is 0.59 ps/s, which agrees with the correction amount of 3×10^{-6}Hz ($\simeq$0.6ps/s) determined by HROG. Standard deviations at this time were 5.4 ns for the code phase and 36 ps for the carrier phase. A large undulation is seen in the residuals of the carrier phase in Fig.4, attributed to poor stability of the synthesizer used to create the carrier frequency for signal transmission (2,656.390 MHz).

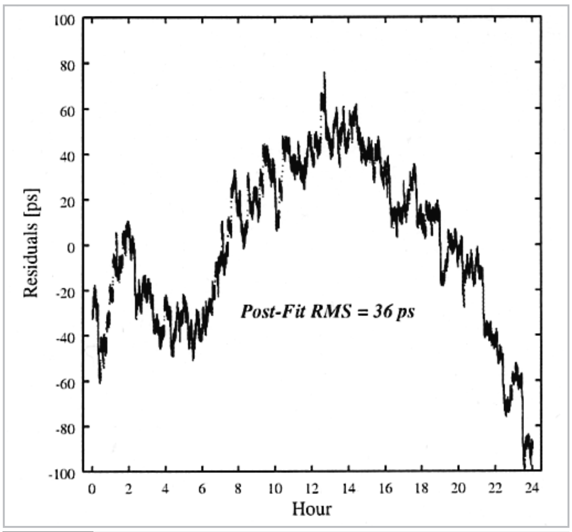

Fig.4 *Residual after the least-square liner fit on measured values of the carrier phase*

2.3.2 Carrier phase ambiguity resolution

In time transfer using the carrier phase, precision in ambiguity resolution defines the precision of comparison, in addition to observation precision. Carrier phase ambiguity resolution consists of two steps: calculation of a float solution by the method of least squares, and conversion of the obtained float solution to an integer. If the float solution can be converted to an integer, the precision of comparison cited in the previous section can be attained.

With GPS, the float solution can be converted to an integer using the double difference observables, whereas with TCE, only the float solution can be obtained due to the use of a single satellite. If this solution cannot be converted to an integer, the solution may feature error resulting from the offset between the float solution and the integer solution at the time of reapplication of the power supply. Since the period of a single round of observation is determined in experimental design, the deterioration in precision resulting from carrier phase ambiguity becomes a problem in extended time transfers.

Obtaining a float solution is accomplished by solving observation formulas (4) and (7). Since internal delay is considered to be nearly constant, it may be ignored in a discussion of comparison precision. Therefore, error attributable to ionospheric effects and observation error of the code phase determine the precision of carrier phase ambiguity resolution. Since the two observations are the same (with the exception of the influence of the ionosphere), estimation precision can be improved by time averaging.

Based on the results of the previous section, the observation precision for the code phase is approximately 5 ns. One-hour averaging can increase the observation precision to approximately 80 ps. Note that it is essential that no cycle slip occurs in the carrier phase during averaging. Such slipping is considered unlikely, as the ETS-Ⅷ will be in a geostationary orbit, and also because both the satellite and Earth stations will employ parabolic antennas.

The effect of the ionosphere remains problematic. This effect can be determined using dual-frequency observations and by applying a frequency dispersion characteristic[2]. However, since the ionospheric delay determined from the code phase observation has a high-frequency component that depends on the observation error of the code phase, this method of determining the ionospheric effect will reduce the precision of ambiguity resolution. In this case it is necessary to increase precision using a process involving the following iterated procedures.

Initially, ionospheric delay determined from the code phase observations is used; after the carrier phase ambiguity resolution with some precision, ionospheric delay is found using the carrier phase observations, and the carrier phase ambiguity resolution is determined using this new value.

3 Time transfer experiment

3.1 Onboard atomic clock

The evaluation of the performance of an onboard atomic clock is one of the major objectives of the current project. Since precision in determination of the offset of an atomic clock influences positioning accuracy, determining the difference between UTC(CRL) and HAC with high precision will have a significant impact on the positioning mission. Here it is important to note that there are no precedents in the determination of long-term performance of both onboard and ground clocks (with the exception of LASSO), and we can thus affirm that current research represents the most advanced experimentation of its kind. With LASSO, the stability of the onboard clock was about 10^{-10} /day, due to the use of a quartz oscillator. Since HAC employs a cesium clock, stability is better, at $10^{-11}/\sqrt{\tau}$.

It is well-known that the proper time of the clock is related to geocentric coordinate time (TCG), which depends on the gravitational potential of the Earth[7][8]. In HAC, the clock is slowed by a frequency of 5.5×10^{-3}Hz to allow for this gravitational effect. It is anticipated that the highly precise time transfer available using TCE will prove effective in verifying such predictions of the general theory of relativity.

3.2 Two-way time transfer via TCE

TCE can perform two-way satellite time transfer between a fixed station and a portable station. In two-way satellite time transfer using communication satellites deployed to determine international atomic time, the carrier phase of an Earth station subject to time transfer cannot be used, as the oscillator aboard the satellite is employed to conduct frequency conversion for UPLINK and DOWNLINK. On the contrary, TCE performs time transfer between HAC and an Earth station using the carrier phase, resulting in inter-station precision as high as approximately ±100ps.

Two-way satellite time transfer permits highly precise time transfer, regardless of the positions of the satellite and the Earth station, through the mutual transmission of signals between two stations. However, in practice differences may arise between signal propagation paths due to the influence of the Earth's rotation. In a rotating frame, the correction term δ, representing the time required for a signal transmitted from satellite $\boldsymbol{x}_{ra}$ at time t_0 to arrive at Earth station $\boldsymbol{x}_{rb}$ at time t_1, is expressed by formula (8)[9].

$$\begin{aligned} T &= \frac{R_0}{c} + \delta \\ &= \frac{R_0}{c} - \frac{U_g R_0}{c^3} + \frac{\boldsymbol{R}_0 \cdot \boldsymbol{v}_b}{c^2} + \frac{R_0}{2c^3}\left[v_b^2 + \boldsymbol{R}_0 \cdot \boldsymbol{a}_b + \frac{(\boldsymbol{R}_0 \cdot \boldsymbol{v}_b)^2}{R_0^2}\right] \\ &\quad + \frac{2GM_E}{c^3} \ln\left[\frac{x_{rb} + \boldsymbol{R}_0 \cdot \boldsymbol{x}_{rb}/R_0}{x_{ra} + \boldsymbol{R}_0 \cdot \boldsymbol{x}_{ra}/R_0}\right] \end{aligned} \qquad (8)$$

Here, U_g stands for the gravitational potential on the geoid surface; R_0 stands for the vector from the satellite to the Earth station in the rotating frame; $\boldsymbol{v}_b$ represents the velocity vector of the Earth station in an inertial frame; $\boldsymbol{a}_b$ is the acceleration vector of the Earth station in the inertial frame; G is the gravitational constant; and M_E represents the mass of the Earth.

Note that this correction term does not take into consideration any quantity of 1 ps or less. The second through fourth terms on the right side of formula (8) originate from the frame difference and represent the Sagnac effect. The last term depends on the gravitational potential. In two-way satellite time transfer using a geostationary satellite, calculation can be performed assuming the distance between the satellite and the Earth station $\boldsymbol{R}_0$ to be constant, and consequently the c^1 term and the c^3 term are canceled out by propagation from the satellite to the Earth station and from the Earth station to the satellite. Similarly, the term that depends on the gravitational potential is canceled out because the displacement from the satellite to the Earth station and that from the Earth station to the satellite are the same. As a result, $(\boldsymbol{R}_0 \cdot \boldsymbol{v}_b)/c^2$ remains as the correction term.

The two-way satellite time transfer network[10] within the Asian region (a network for which the CRL is responsible) includes a link with Australia (AUS) via PAS8 and a link with Taiwan (TL) and China (NTSC) via JCSAT; the Sagnac correction for these links are as shown in Table 1. In actual observation, it is generally difficult to isolate and identify the influence of the Sagnac effect, as it is impossible to separate the influence of this effect from the time difference between the clocks of two stations. By incorporating the TCE Earth station in the existing network, the time difference between two stations can be determined from a comparison of TCE and communication satellite observation results. Since two sets of results are obtained (corresponding to different satellite configurations with common reference signals), the Sagnac correction can be determined from the difference in these two sets of results. It is expected that the Sagnac correction may be verified in actual measurement by comparing the difference with the value calculated by formula (8).

Table 1 *Sagnac correction quantities for the two-way satellite time transfer network in the Asian area*

CRL and	Sagnac 補正	Satellite
AUS	43.86 ns	PAS8
NTSC	−85.29 ns	JCSAT 1B
TL	−63.07 ns	JCSAT 1B

3.3 Comparison of ranging technology between laser and radio signals

The values observed using TCE enable determination of the round-trip distance between the satellite and the Earth by summing the formulas (5) and (6). Expressing the distance between the satellite and the Earth station as $\rho_r^s(t, t-\tau_r^s)$ and the internal delay as $\delta_r' = \delta_s^r + \delta_r^r$, $\delta_s' = \delta_s^s + \delta_r^s$, formula (9) is derived.

$$\begin{aligned}\Phi_r(t) + \Phi^s(t) \quad = \quad & 2\rho_r^s(t, t-\tau_r^s) \\ & -\{I_d + I_u\} + 2T + c(\delta_r' + \delta_s') \\ & +\lambda_d[\phi_r(t_0) - \phi^s(t_0) + N_r] \\ & +\lambda_u[\phi^s(t_0) - \phi_r(t_0) + N^s] \\ & +\varepsilon_r^s \end{aligned} \tag{9}$$

ETS-Ⅷ is capable of SLR observation, and the CRL intends to track ETS-Ⅷ from its SLR observation station[11]. It will be possible to observe the difference in laser ranging and radio-wave ranging by installing a portable station at nearly the same position as that of the SLR station and observing SLR and TCE simultaneously. Since atmospheric propagation delay differs significantly depending on the use of light or radio waves, it is assumed that the results of simultaneous observation will enable us to evaluate the relative effects of hydrostatic delay and wet delay, the influence of the ionospheric delay, and more.

However, with the increase in unknowns [as seen in the comparison between formulas (7) and (9)], carrier phase ambiguity resolution becomes more difficult than time transfer. Moreover, comparison between absolute values becomes important when performing comparison with SLR; however, TCE is structurally incapable of determining the absolute value of internal delay, and hence generates an offset in such comparison. How these values should be estimated in the future represents a practical analytical challenge.

4 Concluding remarks

The space-borne time comparison mission represents pioneering research, in which atomic clocks aboard a satellite and on the ground are measured with precision of approximately a few tens of ps. At the same time the CRL has also been pursuing the development of a space-borne hydrogen maser atomic clock, and we believe that long-term observation of an atomic clock in orbit will provide important basic data for the development of such atomic clocks. Moreover, since the establishment of a proprietary navigation satellite technology is currently a national goal, highly precise time synchronization between satellites and the ground is becoming increasingly important. For this and many other reasons, we believe that the collection of basic data and the establishment of an appropriate analytical technique are accomplishments of the greatest importance.

Acknowledgements

We would like to thank the members of the ETS-Ⅷ Project Team and Office of Satellite Technology, Research and Applications, Satellite Mission Operations Department, National Space Development Agency of Japan, for their cooperation in the course of TCE development and testing.

References

1 M. Homma, S. Yoshimoto, N. Natori, and Y. Tsutumi, "Engineering Test Satellite-8 for Mobile Communication and Navigation Experiment", IAF, No. IAF-00-M.3.01, pp.256-263.

2 Y. Takahashi, M. Imae, T. Gotoh, F. Nakagawa, H. Kiuchi, M. Hosokawa, M. Aida, Y. Takahashi, H. Noda, and S. Hama, "Time Comparison Equipment for ETS-Ⅷ Satellite, -Part 1 Development of Flight Model-", This Special Issue of CRL Journal.

3 P. Fridelance and C. Veillet, "Operation and data analysis in the LASSO experiment", Metrologia, 32, pp.27-33, 1995.

4 E. Samain and P. Fridelance, "Time Transfer by Laser Link (T2L2) experiment on Mir", Metrologia, 35, pp.151-159, 1998.

5 M. Imae, T. Suzuyama, T. Gotoh, H. Shibuya, F. Nakagawa, N. Kurihara, and Y.Shimizu, "Two Way Satellite Time and Frequency Transfer", This Special Issue of CRL Journal.

6 P.J. Teunissen and A. Kleusberg, GPS for Geodesy, 2nd Edition, Sec. 5, Springer, 1998.

7 M. Hosokawa, "Four Dimensional Space-Time and Reference Frame", Review of the Communications Research Laboratory, Vol. 45, Nos.1/2, pp.3-18, March/June 1999. (in Japanese)

8 P. Wolf, and G. Petit, "Relativistic theory for clock syntonization and the realization of geocentric coordinate times", Astron. Astrophysics, 304, pp.653-661, 1995.

9 G. Petit, and P. Wolf, "Relativistic theory for picosecond time transfer in the vicinity of the Earth", Astron. Astrophysics, 286, pp.971-977, 1994.

10 S. Hongwei, M. Imae, and T. Gotoh, "Performance of Two-way Satellite Time and Frequency Transfer in Asia-Pacific Region", Journal of the Geodetic Society of Japan, Vol.49, No.2, pp.135-142, 2003.

11 H. Kunimori, K. Imamura, F. Takahashi, T. Itabe, T. Aruga, and A. Yamamoto, "New Development of Satellite Laser Ranging System for Highly Precise Space and Time Measurements", Journal of the Communications Research Laboratory, Vol.38, No.2, pp.303-317, 1991.

GOTOH Tadahiro

Reseacher, Time and Frequency Measurement Group, Applied Research and Standards Division

GPS Time Transfar

***HOSOKAWA Mizuhiko**, Ph. D.*

Leader, Atomic Frequency Standards Group, Applied Research and Standards Division

Atomic Frequency Standards, Space Time Measurements

***NAKAGAWA Fumimaru**, Ph. D.*

Research Fellow, Time and Frequency Measurements Group, Applied Research and Standards Division

Satellite Navigation, Satellite Time Transfer

TAKAHASHI Yasuhiro

Senior Researcher, Time and Frequency Measurements Group, Applied Research and Standards Division

Satellite Communication, Satellite Positioning System

***FUJIEDA Miho**, Ph. D.*

Research Fellow, Time and Frequency Measurements Group, Applied Research and Standards Division

Satellite Navigation, Precise Time Transfer

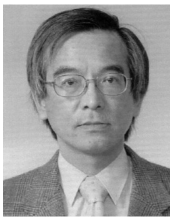

IMAE Michito

Leader, Time and Frequency Measurements Group, Applied Research and Standards Division

Frequency Standards

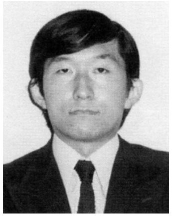

***KIUCHI Hitoshi**, Dr. Eng.*

Senior Researcher, Optical Space Communications Group, Wireless Communications Division

Radio Interferometry, Optical Space Communication

AIDA Masanori

Senior Researcher, Research Planning Office, Strategic Planning Division

Frequency and Time Standards

TAKAHASHI Yukio

Senior Researcher, Keihanna Human Info-Communication Research Center, Information and Network Systems Division

Posting Technology, Astrometry, VLBI